

## Chaff Tagging for Tracking the Evolution of Cloud Parcels

Roger F. Reinking<sup>1\*</sup>, Roelof T. Buintjes<sup>2</sup>, Bruce W. Bartram<sup>1</sup>, Brad W. Orr<sup>1</sup>, and Brooks E. Martner<sup>1</sup>

<sup>1</sup>NOAA/ERL/Environmental Technology Laboratory, Boulder, CO

<sup>2</sup>Research Applications Program, National Center for Atmospheric Research, Boulder, CO

**Abstract.** A means to mark and track a moving and mixing volume within a cloud is useful for estimating the transport and dispersion of seeding material or other aerosols and thus for determining where and when the microphysical effects of the aerosols should occur. A proven approach has been to release and track chaff into a cloud and track it with circular polarization radar to estimate the rates of dispersion, loft, and dilution of ingested aerosol, as well as the filling of the cloud volume. The chaff, an effective tracer, is separable from the cloud because it strongly depolarizes the radar's signal. A primary disadvantage of this cloud-volume-filling approach is that radar measurements of the microphysical evolution of the tracked cloud parcels may be masked by the chaff itself. To measure transport and dispersion in cloud and simultaneously unambiguously examine the microphysical evolution in the same volume, a refined approach was devised to tag but not fill the cloud volume with chaff. Several experimental designs for chaff tagging are proposed for stratiform or gravity-wave clouds, and for cumuliform clouds. The tagging technique will be more difficult to apply in convective clouds and is not yet tested. However, a "parallel lines" experiment designed for stratiform clouds was tested with hygroscopic seeding in a wave cloud with intrusions of convective cloud. The chaff lines were tracked for about one hour despite some ingestion by convective elements. This demonstrated that a seeded cloud volume could be bracketed and tracked effectively. A hygroscopic seeding signature, anticipated to appear as a line of enhanced reflectivity along a seeded flight path between the chaff lines, was not detected. A "tagged circle" experiment with silver iodide seeding was conducted in a precipitating wave cloud. A seeded circle was tagged with arcs of chaff, allowing it to be tracked efficiently. A seeding effect was indicated along the circular seeded path between the chaff arcs as signatures of enhanced reflectivity and values of depolarization indicative of pristine, new ice crystals. The results of these experiments demonstrate the potential of the chaff tagging technique.

### 1. INTRODUCTION

Hobbs et al. (1981) demonstrated that a standard radar measuring only reflectivity could be used to detect snow plumes generated by seeding supercooled stratus with dry ice from an aircraft. That study had the advantage of simplicity. A shallow (1-2 km deep), very uniform, all-liquid cloud was advecting over a vertically pointing 8.6 mm radar. Although penetrations of the seeded track with the instrumented aircraft did document the presence and concentrations of the resulting ice particles, the study was at a disadvantage due to the lack of radar volume scanning and a means to explicitly mark and track the space-time evolution of the whole seeded

track. In most situations, the cloud dynamics and microphysics are more complicated, so a means to mark and track the seeded cloud volume provides a very strong advantage for estimating the transport and dispersion of seeding material and the consequent microphysical effects of seeding.

A technique called TRACIR (Tracking Air with Circular-polarization Radar) has proven useful for tracking parcels of air and measuring the time-history of cloud volume filling by aerosols such as seeding material within both convective and stratiform clouds (Martner and Kropfli 1989, Martner et al. 1992, Reinking and Martner 1996, Stith et al. 1996). Chaff, the material that is tracked, is comprised of aluminum-coated glass filaments about 25  $\mu\text{m}$  in diameter that can be dispersed in great numbers and are designed to be detected by radars with circular polarization. Chaff filaments approximately circulate and mix with the air, since their settling rate is only  $\sim 0.25 \text{ m s}^{-1}$ .

---

\*Corresponding author's address: Dr. Roger F. Reinking, NOAA/ERL/ET6, 325 Broadway, Boulder CO 80302; rreinking@etl.noaa.gov.

The detectability of chaff is enhanced by cutting the filaments to half the wavelength of the tracking radar to make them resonant dipoles with large radar cross sections. Chaff can be cut to the appropriate length as it is released from an aircraft or the ground. Depolarization rather than the reflectivity of a radar's signal is used to detect the chaff inside clouds. Our experience indicates that chaff in the high concentrations that immediately follow release will have reflectivities of ~20 dBZ, and that these reflectivities will diminish with dilution. Therefore, the reflectivity of chaff normally becomes partially or totally obscured by the cloud reflectivity, but strong depolarization of the radar's signal by the chaff fibers allows them to be detected within a field of higher reflectivities.

The orientation of the fibers does not affect the signal, nor hence, derived concentrations, if the observing radar uses circular polarization. The effect is measured as the circular depolarization ratio (CDR), which is the ratio of energy returned in the radar's receiving cross channel to energy returned in the main channel from a circularly polarized signal transmitted in the main channel. Theoretically, for chaff in clear air, CDR = 0 dB. This depolarization value is quite different from that caused by hydrometeors other than hail. In practice, chaff has been identified with CDR values ranging from +4 to -14 dB, in clouds with reflectivities up to 30-35 dBZ (e.g., Reinking and Martner 1996). The lesser (more negative) depolarizations usually result from dilution and are identified as chaff by spatial and temporal continuity of the signal. The NOAA/ETL X-band (3.2 cm) circular-dual-polarization Doppler radar was used in the noted studies that detail TRACIR, and in the present study.

The standard approach has been to release the chaff filaments along with seeding material from an aircraft or the ground, to follow the transport, dispersion and cloud volume filling by both. Alternatively, chaff is released alone to examine how seeding material might disperse within a certain type of cloud if it were to be seeded, for example, or how pollutants might be ingested from the planetary boundary layer. This approach provides measures of the rates of dispersion, loft, and dilution of the ingested material, as well as the volume filling. (In this paper, "volume filling" refers to the volume of a cloud rather than radar-beam filling, except as noted.) A primary disadvantage of this approach is that radar measurements of the microphysical evolution of the tracked volume may be masked by the chaff itself. Microphysical evolution can be measured as changes in cloud reflectivity, or with

more specificity as changes in cloud depolarization. Reflectivity,  $Z_e$ , measures the combined effect of hydrometeor size and concentration. However, chaff does have reflectivity, and although this reflectivity is usually slight enough to be obscured by the cloud's reflectivity, it may still contaminate or at least introduce some uncertainty in reflectivity as a measure of microphysical evolution. A general depolarization ratio may be defined as

$$DR = 10 \log (P_{cr} / P_{co})$$

where  $P_{co}$  is the power returned in the main channel and  $P_{cr}$  is the power returned in the cross channel. Any of various DRs are determined by hydrometer shape, settling orientation, and bulk density, and the polarization state of the transmitted radiation (circular, linear, elliptical). Therefore, the DRs can provide estimates of hydrometeor type or phase (ice vs. liquid), and the evolution thereof (Reinking et al. 1996, 1997). Chaff is tracked by measuring CDR, so any measure of the hydrometeor type or phase using CDR or related polarization parameters in the same cloud volume introduces some ambiguity into hydrometeor identification unless the values of CDR characterizing the hydrometeors are substantially different from the values of CDR characterizing chaff. For some ice particle types the difference is substantial; for others it is not. The differentiation can be enhanced via measurement with a radar of significantly different wavelength than that for which the chaff length is cut. This approach can be useful, but it is tricky.

To optimally measure transport and dispersion in cloud via TRACIR and simultaneously examine microphysical evolution, a modified experimental design is required. One approach might be to pair similar clouds with proximity, releasing chaff into one and not into the other, under the assumption that each cloud of the pair will behave similarly without seeding, and similarly with seeding if both clouds are treated. The standard volume-filling approach to chaff tracking would be employed in one cloud to measure loft and dispersion, and the other would be examined with a radar for microphysical evolution, assuming loft and dispersion of seeding material in this cloud would be similar to that in the one with chaff. In this version of a target/control experiment, both clouds of the pair would be seeded, or not seeded, but chaff would be released only into one. A sufficient sample of cloud pairs would then be gathered to statistically compare the seeded and unseeded cloud pairs.

Another approach, with fewer assumptions and more control over the experiment, is that of chaff tagging. The concept and initial experiments that

demonstrate chaff tagging are described here. The experiments were conducted during the 1995 Arizona Program (Klimowski et al. 1998) in storm-embedded orographic gravity wave clouds.

## 2. EXPERIMENTAL DESIGNS FOR CHAFF TAGGING

A refined approach to the use of TRACIR is to tag but not fill the cloud volume with chaff. The presumption is that the volume of interest can still be tracked by following the chaff tags, and microphysical changes simultaneously can be monitored in the same cloud volume, between or near the tags, to avoid confusion with the chaff.

### 2.1 Designs for Stratiform Clouds

Two designs for monitoring seeding effects in stratiform clouds, including gravity wave clouds, are as follows.

Tagged circle. Using flares burning on wing racks or continuous-burning wing-mounted aerosol generators, an aircraft can seed around a complete circle in an advecting stratiform cloud, but simultaneously release chaff only on two arcs of the circle. Radar can then track the circle measuring the depolarization caused the chaff tags (i.e., their CDR signature), while simultaneously measuring the reflectivity ( $Z_e$ ) changes due to seeding along the whole circle but particularly in the gaps between the chaff tags. This experiment might be enhanced by measuring changes in depolarization due to ice or enlarged drops caused, respectively, by glaciogenic or hygroscopic seeding. Since depolarization signatures are the order of 10 dB down from reflectivity signatures, the latter approach would be most effective if a shorter wavelength (e.g.,  $K_a$ -band; 8.66 mm) radar were used to gain a higher sensitivity to the new, growing hydrometeors. This might be accomplished with an additional, synchronized radar or a dual-wavelength radar.

Parallel lines. Figure 11 in Klimowski et al. (1998) illustrates a well-defined line of chaff detected in CDR in a wave cloud. Similarly, parallel lines of chaff can be dispersed by an aircraft to bracket a seeding line where microphysical changes may be monitored as above. The chaff lines will advect with the cloud volume to continuously mark and isolate the position of the bracketed seeded line.

In the tagged circle or parallel lines experiments, the chaff tags or "brackets" should allow radar to unambiguously identify, follow, and monitor

the treated region in clouds of a stratiform nature. Experiments of each of these types are described below.

### 2.2 Designs for Convective Clouds

Chaff tagging to isolate and monitor seeded volumes will be more difficult in convective clouds because of the more vigorous mixing. However, some potentially useful designs can be conceived.

Trailing plume tag. For cloud-base seeding in convective cloud updrafts, Reinking and Martner (1999) proposed that it might be possible to release a burst of chaff, cease the chaff release for several seconds, and release a second burst of chaff, seeding throughout. The chaff would mark the leading and trailing portions of the seeding cloud volume as carried by the updraft, and the induced microphysical changes between the marks could be monitored with the radar's  $Z_e$  and DR measurements without interference from the chaff. Under further scrutiny, this approach is weakened by the fact that the loft of chaff from a given release in an updraft is not complete, immediate and isolated; rather, the entrainment is gradual and continuous, such that the chaff leaves a trail to cloud base (Reinking and Martner 1996). The necessary modification to tagging updrafts is therefore to seed well into an updraft, and then mark the end of the seeded plume with a burst of chaff. The chaff will then show the loft and mark the lowest reaches of the seeded zone. Figure 1a shows the reflectivity of an orographic cumulus cloud; Fig. 1b shows a strong signature of a volume of the updraft in that cloud with a clearly defined top and filled with chaff (discussed as Fig. 10a,b in Klimowski et al. 1998). The tagging concept is that the updraft in the cloud just above this chaff top may be inspected for microphysical changes due to seeding in the updraft just before chaff is released, such that the chaff follows the seeding material and its microphysical effects. The same approach might be attempted in seeding the tops of rising turrets from wing-mounted generators. Transport within and circulating around the turrets could be estimated in this way.

Flare curtain tags. Convective clouds are often seeded from their tops by releasing a curtain of droppable flares from an aircraft. In the Florida Area Cumulus Experiment (FACE), for example, cloud physics aircraft following a seeding aircraft through a convective updraft often did not find a seeding signature (in the form of high concentrations of ice crystals). Based on updraft speeds and the time elapsed between an aircraft release of nucleant and

subsequent microphysical sampling, it was hypothesized and inferred from ice particle measurements but never proven that the flare material was rapidly lofted above flight level, such that the microphysical signatures of seeding were to

be found above the sampling altitude. If, while releasing such a curtain of seeding material, the curtain were marked by dropping chaff flares at both ends, the chaff would show the movement and mixing of the seeded curtain, while the microphysical changes could conceivably be monitored between the flares. For comparison in paired clouds, the corresponding volume-filling experiment would be one of releasing chaff flares along with seeding flares across the entire curtain. Chaff flares can be manufactured, and both the tagging and volume-filling experiments are worth doing, due to the extensive use of droppable seeding flares.

In summary, chaff tagging is a customized version of chaff tracking that marks cloud parcels and follows their transport while leaving the treated cloud volume between or adjacent to the tags open for radar examination of the hydrometeor evolution. A number of variations are possible on the suggested experimental designs.

### 3. CHAFF TAGGING EXPERIMENTS

Chaff tagging experiments were conducted in gravity wave clouds during The 1995 Arizona Program. The operational area is shown in Fig. 1 of Klimowski et al. (1998). The nature of the wave clouds is described by Brientjes et al. (1994) and Reinking et al. (1999). The project cloud physics and chaff release aircraft, a Cheyenne II from Weather Modification, Inc., was based in Prescott, southeast of the project area. The NOAA/ETL dual-polarization (circular) X-band (3-cm) Doppler radar was used to apply TRACIR. It was located on the airport grounds at Cottonwood, at 1076 m AGL, in the Verde Valley, between the Black Hills and the Mogollon Rim. Mingus Mountain and the Black Hills form a NW-SE ridge immediately southwest and normally upwind of the Verde Valley watershed. The Mogollon Rim rises from the northern and northeast reaches of the Verde Valley and is the primary recipient of precipitation associated with orographic wave clouds, and the potential target area for precipitation enhancement by seeding (Brientjes et al. 1994, Reinking et al. 1999). The two chaff tagging experiments described in the next sections demonstrate the technology as it was applied in this scenario.

### 4. A "PARALLEL LINES" TAGGING EXPERIMENT

A "parallel lines" chaff tagging / hygroscopic seeding experiment was conducted in a gravity wave cloud on 14 February 1995. The gravity wave had induced a well-developed foehn gap and a wave cloud

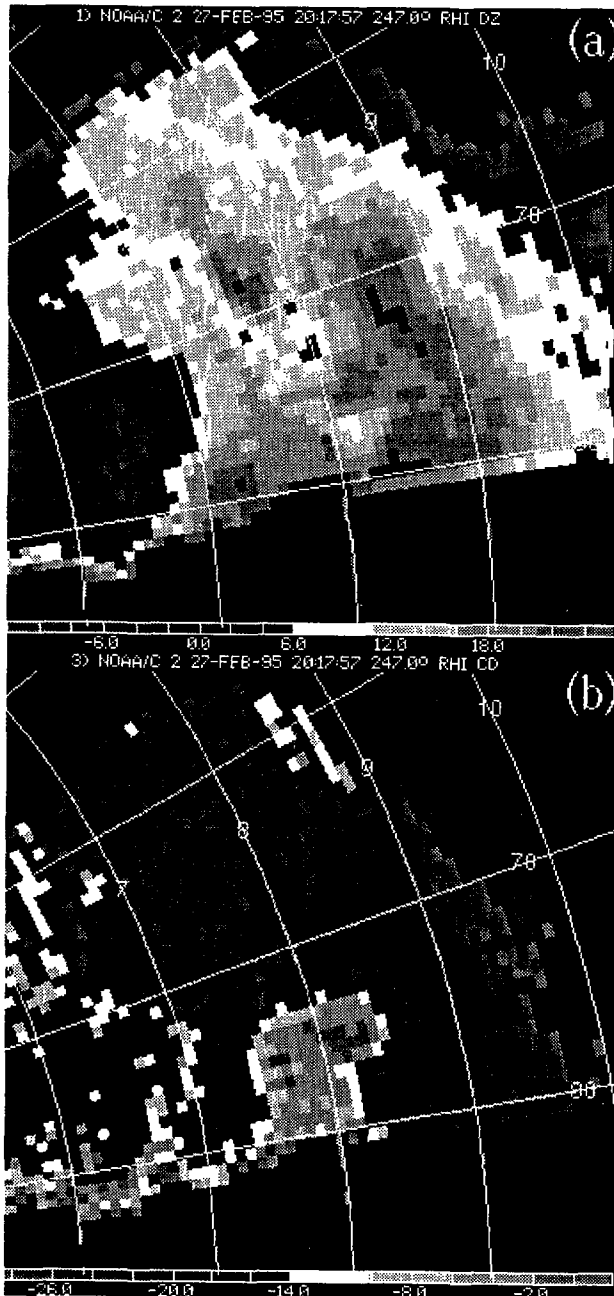


Fig. 1. Radar RHI scan showing the vertical cross-section of an orographically generated cumulus cloud. (a) the reflectivity ( $Z_e$ , dBZ) is greatest in the rainshaft, which is adjacent to (b) the updraft, clearly defined in CDR (dB) as it is filled with chaff (from Klimowski et al. 1998).

deck downwind of the gap. The chaff release/seeding aircraft flew at wave-cloud base in the downwind edge of the gap. All airborne releases were made at  $\sim 2.4$  km (8000 ft) MSL and 1.4 km AGL relative to Cottonwood Airport, approximately along the  $140^\circ$  radial from the radar, and across the wind. First, the aircraft released a line of chaff, and this began to be advected toward the northeast. Then, the aircraft reversed heading and a line was seeded with hygroscopic (NaCl) flares along the same radial. The aircraft reversed heading a second time, and a third line, this one of chaff, was released along the same radial. Thus, as one line was advected away from the release radial, it was replaced by another, to bracket a seeded line with two chaff lines. A log of these events and the detection of the chaff is presented in Table 1. The midway point of the seeding leg establishes a reference time of  $t_0 = 0047$  UTC.

**Table 1. Log of controlled events and detection of chaff lines (UTC) for 14 February 1995 experiment.**

0040-0044	$\sim 4$ min chaff release, 1 <sup>st</sup> line.
0042	First radar detection of chaff.
0045-0049	$\sim 4$ min seeding line, 6 flares.
0047	Reference time, $t_0$ .
0050-0056	$\sim 6$ min chaff release, 2 <sup>nd</sup> line.
0057-0102	Both chaff lines now very visible in sector scans.
0121	Chaff lines moving over Mogollon Rim.
0137	Last detection of chaff.

The clouds that persisted through this event are illustrated by the 004929 UTC ( $t_0 + 2$  min) RHI scan in Fig. 2, made with a second, cloud-sensing  $K_a$ -band radar. The experiment was conducted in the cloud system below 4 km AGL, not the overriding wave at 5-7 km AGL. At the lower level, the air in the gravity wave was descending down the mountain slope (from the left in the figure) and created a hydraulic jump just upwind of the radar. Beyond the foehn gap, this resulted in lift of as much as  $\sim 4$  m  $s^{-1}$  and produced a low-level wave cloud which overrode small convective elements. The convective elements are evident and the wave cloud developed soon after 0059 UTC (Fig. 2a). The convection was also driven by the cross-valley gravity wave flow, which forced lifting up the next slope toward the Mogollon Rim. In the vicinity of the radar, a rotor developed, the return flow of which is evident in the velocity measurement (Fig. 2b). The low-level gravity wave cloud was quite

diffuse ( $\sim -22$  dBZ) compared to the convective elements ( $\leq +10$  dBZ). The wind in the wave reached  $\sim 8$ -10 m  $s^{-1}$  from  $\sim 225^\circ$ , from a  $K_a$ -band velocity

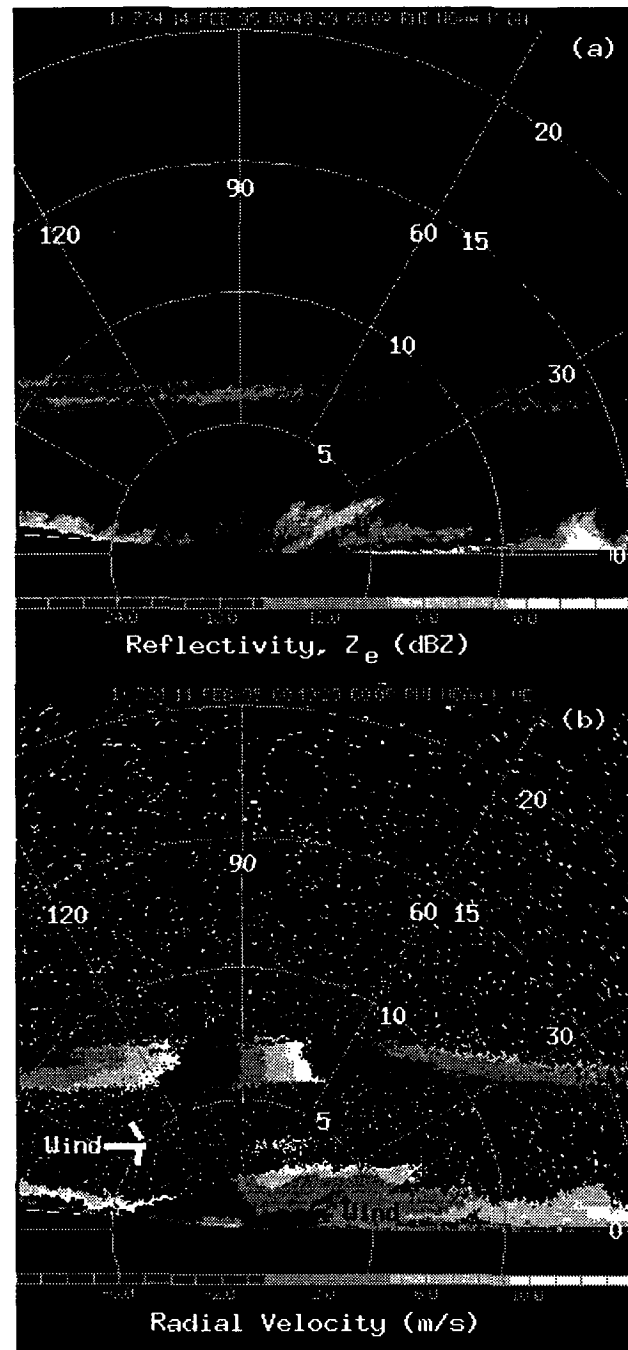


**Fig. 2. Over-the-top radar RHI scan of (a) cloud reflectivity ( $Z_e$ , dBZ) and (b) radial velocity ( $V$ , m  $s^{-1}$ ) from  $60^\circ$  azimuth at right (004929 UTC,  $t_0 + 2$  min, 14 Feb 1995). Positive values of velocities indicate flow away from the radar. The wind was generally left-to-right except in return flow of the wave's rotor at the lowest levels.**

azimuth display (VAD) scan at 0058 UTC. Undulations in the wave governed cloud top across the valley. In all, the system was much more complex than a stratiform wave cloud.

Each of the two chaff lines was visible in the CDR measurement within a minute after completion of their release into this cloud system. Fig. 3a shows both lines at 010120 UTC ( $t_0 + 14$  min), as indicated by the signatures in  $\text{CDR} \geq -5$  dB. None of the clouds was producing returns at  $-10 \text{ dB} \leq \text{CDR} \leq +2$  dB. Both lines were intact. The initial, northernmost chaff line (Table 1) had advected 12–13 km northeastward from the release radial, and the second chaff line had advected 6–7 km from that radial. By this time, dispersion was greater in the first line, due to its longer exposure after release. In the radar reflectivity, the chaff lines could generally be distinguished from the low reflectivity clouds that filled the space between them, but not from the heavier echo of the convective elements at the east and west ends of the lines (Fig. 3b). Just 2.5 min later, the northern chaff line began to be ingested into the convection, as indicated by a rapid widening of the line associated with convective elements.

The involvement with both the wave and the convection continued, eventually involving and widening the dispersion of both lines (011120 UTC or  $t_0 + 24$  min; Fig. 4a, b). A low-elevation RHI scan at 011355 UTC ( $t_0 + 27$  min) from horizontal to  $15^\circ$  elevation toward the  $34^\circ$  azimuth sliced vertically through portions of both lines (Fig. 5a,b); this shows that the chaff was lofted as high as 2.5 km AGL (about 1.1 km above the altitude of release in the foehn trough) in the convection, and stretched northeastward by the wind through the wave. Also, downwind, some of the chaff was driven back to lower altitude, evidently by the undulating wave action. By 0122 UTC, some of the southernmost line was still distinguishable as a chaff area some 5 km wide, but most of it was more widely dispersed in the combined convection and wave action and still highly visible in CDR, primarily between 10 and 40 km range along the  $20^\circ$  radial (not shown). The two lines were no longer separable.

In several plan position indicator (PPI) sector scans, there are possible hints of reflectivity enhancement along the seeded line, as bracketed between the two chaff lines (e.g., just north of the  $90^\circ$  radial at 10–13 km range in Fig. 3b). However, any seeding signature from enhanced drop concentrations was too subtle to positively identify against the highly non-uniform background of the existing clouds. In data processing, CDR was re-

scaled from the  $+2 - -14$  dB range for identifying chaff, to a  $-10 - -40$  dB range to determine depolarizations by cloud particles, following the small chance that a line of no depolarization would be evident. Spherical drops like those that would be

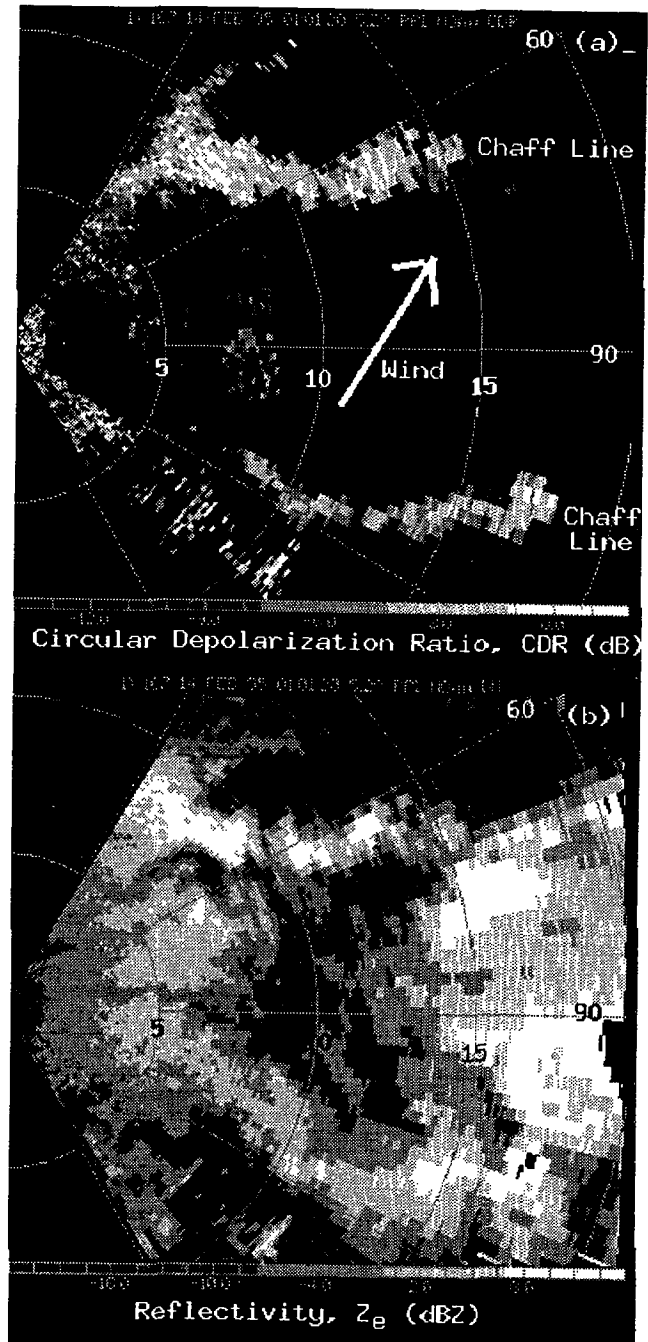


Fig. 3. X-band radar PPI sector scan at  $t_0 + 14$  min through  $90^\circ$  azimuth at  $5.2^\circ$  elevation of (a) CDR (dB) showing chaff lines and (b) corresponding cloud  $Z_e$  (dBZ). (5 km range rings; 010120 UTC, 14 February 1995.)

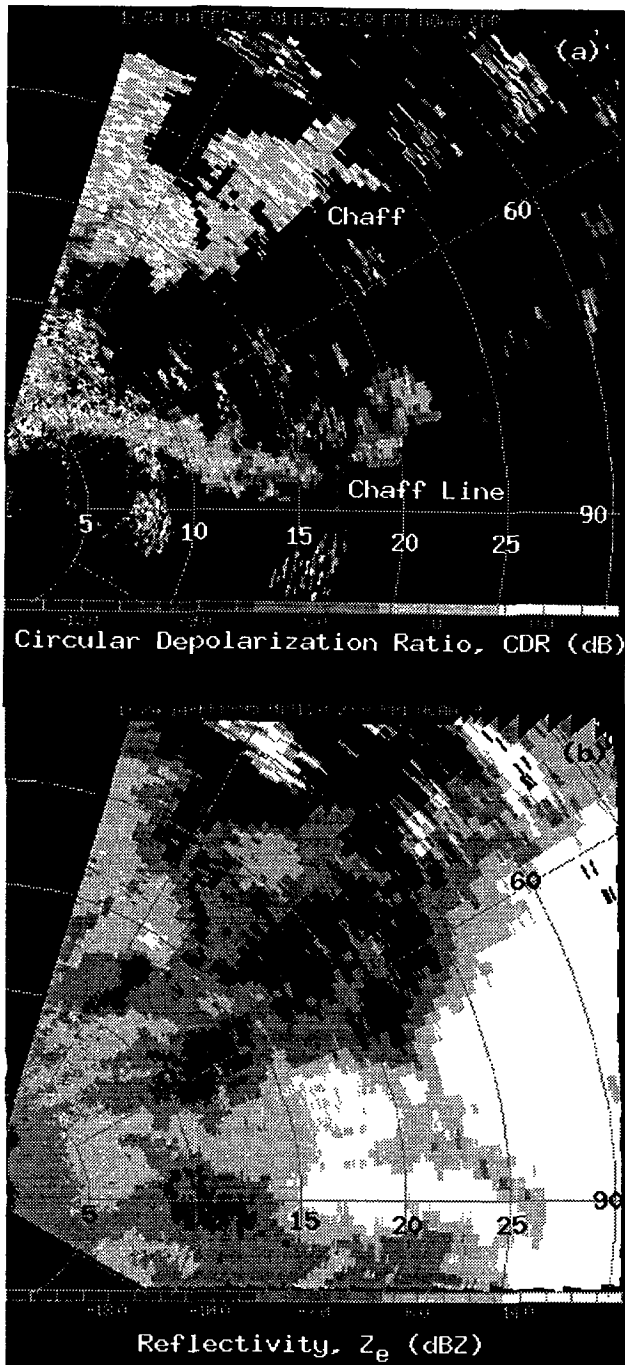


Fig. 4. X-band radar PPI sector scan at  $t_0 + 24$  min through much of northeast quadrant at  $2.6^\circ$  elevation of (a) CDR (dB) showing chaff lines becoming involved in convection and (b) corresponding cloud  $Z_e$  (dBZ). (5 km range rings; 011120UTC, 14 February 1995.)

created by hygroscopic seeding cause no depolarization, so their CDR value would be that corresponding to the cross-talk limit of the radar

( $\sim -35$  dB). No measurable CDR signatures were found in the areas between the chaff lines, either to identify a seeded line or complicate its identification. One cannot conclude that the hygroscopics had no effect, only that no effect was definitively observed. This experiment using hygroscopics is obviously difficult, but worth trying again in more uniform clouds. The use of parallel line chaff tagging is well demonstrated, nevertheless, particularly in defining where to look for a seeding effect.

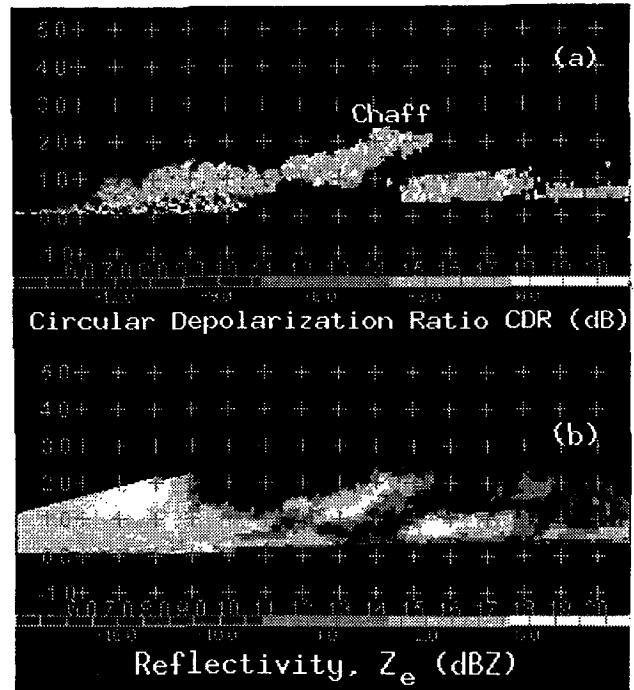


Fig. 5. X-band radar RHI scan from  $0^\circ$  to  $15^\circ$  elevation toward  $34^\circ$  azimuth (at right of figure) of (a) CDR (dB) showing vertical cross section of chaff lines stretched along the wind, and (b) corresponding cloud  $Z_e$  (dBZ). (5 km range rings; 011355 UTC,  $t_0 + 27$  min, 14 February 1995.)

## 5. A "TAGGED CIRCLE" EXPERIMENT

### 5.1 The Tagging and Seeding Operation

A "tagged circle" / AgI seeding experiment was conducted on 6 March 1995 in a purer gravity-wave cloud. This gravity-wave cloud of 4-5 km depth was embedded in the pre-frontal portion of a significant storm. The cloud is illustrated in Fig. 6 just prior to the tagged circle experiment, and the full event is detailed by Reinking et al. (1999). The cloud already contained some ice as well as new liquid water (LW) that was being condensed in the wave's

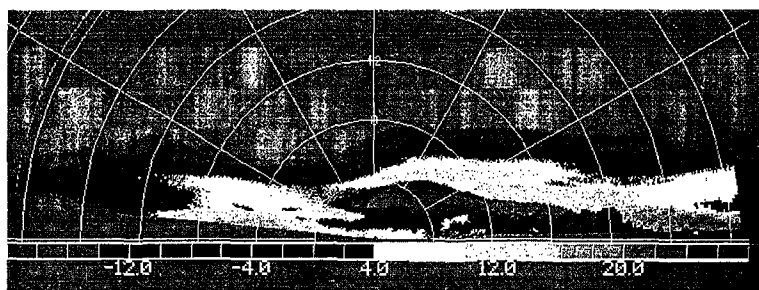


Fig. 6. Reflectivity  $Z_e$  (dBZ) of the gravity wave cloud from an over-the-top RHI scan just prior to treatment with chaff and AgI. The radar position is at center, at zero range (range rings have 4-km spacing).

updraft over Verde Valley. At cloud level near the upwind edge of the updraft, a circular airborne seeding path was marked with two arcs of chaff. While the arcs marked the seeded circle, enhancements in  $Z_e$  of the ring between the arcs were sought to identify enhanced ice concentrations produced by the seeding. Sector-volume scans with the radar were made to follow the tagged and seeded volume. A log of the controlled events for the AgI seeding case and reference times for analysis are presented in Table 2. Mid-points, the times halfway through the seeding and the chaff releases, were

Table 2. Log and reference times (UTC) for controlled events for 6 March 1995 chaff tagging experiment.

Log:

055335-055935	AgI seeding, 1st 5 flares, 6 min.
055720-055825	Chaff release, 1st arc, 1 min 5 s.
055940-060008	Chaff release, 2nd arc, 28 s.
060040-060240	AgI seeding, 2nd 5 flares, 2 min.

Reference times:

055808 $\pm$ 4.5 min	Midpoint and timespan of AgI releases.
055844 $\pm$ 1.4 min	Midpoint and timespan of chaff releases.
055826	Designated reference time, $t_0$ (midpoint of midpoints); $\pm 5$ min for AgI release; $\pm 2$ min for chaff release.

nearly the same, so one reference time,  $t_0$ , has been selected as the "initial time" for both of these events. In-rack, continuous burning flares (pressed composite pyrotechnics, active nucleant AgCL(l), a contact nucleus) were used to glaciogenically seed the wave cloud. The seeding track is shown as a helix in Fig. 7, in ground-relative coordinates. It was approximately circular in coordinates

relative to the mean air motion through the cloud, as substantiated by CDR signatures from the chaff.

Chaff was released along the two arcs of the seeding circle, so as to mark the track but provide gaps in the circle where any seeding signature could be detected with radar without being confused with the chaff. As shown in Fig. 7, seeding was actually conducted over approximately 2.5 revolutions around the circle, so the entire circumference was seeded, despite a 1 min 5 s interval between flare sets. The seeding lasted 9 min 5 s. The upwind, straight-line gap in chaff was about 2.5 km long, and the downwind, straight-line gap was about 4 km long when created.

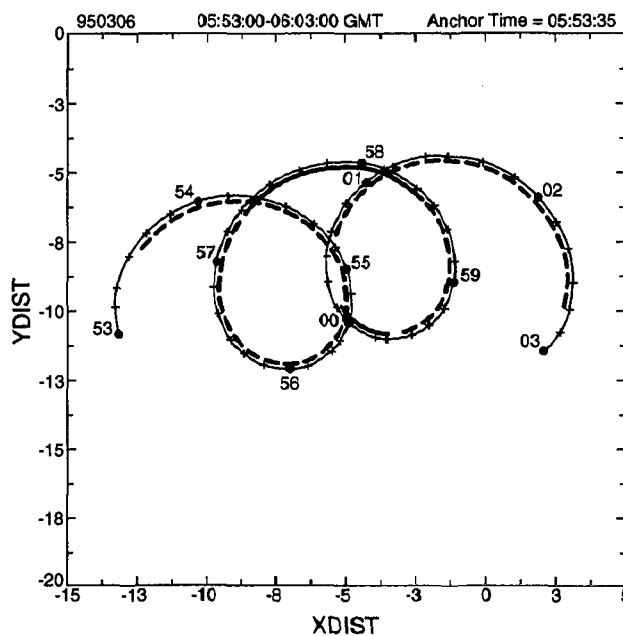


Fig. 7. Aircraft track for the release of chaff (solid) and seeding material (dashed, and solid of north chaff arc) on 6 March 1995, in ground-relative coordinates; distance X,Y (km) is relative to the radar site. The aircraft, flying in a circle, advected with the wind (from Brintjes et al. 1996).



The seeding altitude varied between 4740 and 4910 m MSL, or 3674-3834 m above the radar site at 1076 m elevation; all of the chaff was released between 4750 and 4780 m MSL, or 3675-3705 m AGL. The cloud temperature varied by a few degrees along the seeding track due to an early climb and descent back to a near-constant altitude. The first five flares were burned between  $-6^{\circ}\text{C}$  and  $-8^{\circ}\text{C}$ , where the FSSP liquid water content (LWC) peaked at 0.20 and averaged  $0.03\text{ g m}^{-3}$ . The second five flares were also burned between  $-6^{\circ}\text{C}$  and  $-8^{\circ}\text{C}$ , where LW peaked at 0.02 and averaged  $0.01\text{ g m}^{-3}$  or somewhat less; these values may simply indicate instrument noise. Droplet concentrations, if any, were too small to be measurable (0555-0602 UTC in Fig. 8a-c). Consequently, the initial air temperatures were cold enough, but the drop concentrations and LWC were evidently too small to begin significant nucleation of the seeding agent in the foehn trough, during the

release of material, before being ingested into the updraft where substantial condensation occurred to foster activation of the seeding agent and growth of the resulting ice crystals. In Fig. 8b, the LWC of  $\sim 0.25$  with peaks of  $\sim 0.5\text{--}0.7\text{ g m}^{-3}$  were measured by the aircraft during penetrations through the wave crest (also see Brintjes et al. 1996, Reinking et al. 1999).

## 5.2 Chaff Tracking

The seeding material and chaff were released 5-12 km south of the radar, between 14 km upwind and 3 km downwind of the radar (Fig. 7). Cloud-level advection at this time was  $\sim 20 \pm 2\text{ m s}^{-1}$  toward azimuth  $\sim 80^{\circ}$  (i.e., toward the ENE). The south arc of chaff was detected first, at 060543 UTC ( $\sim t_0 + 7\text{ min}$ ) at  $X, Y = +3\text{ km}, -10\text{ km}$ .

The radar first locked onto both chaff arcs during scan-volume 3, between 061129 and 061214 UTC, respectively 17.3 min and 9.5 min after the beginning and end of the seeding operation, or equivalently, at  $\sim t_0 + 13\text{ min}$ . Since their release, the north and south chaff arcs respectively had broadened to about 1 and 2 km at the radar elevation of strongest return (angle  $\beta = 19^{\circ}$ ,  $\text{CDR} \approx +4 - 8\text{ dB}$ , Fig. 9a); here the centroid of the seeded circle was  $X, Y \approx +12\text{ km}, -6\text{ km}$ , at 13 km range and  $\sim 4.3\text{ km}$  AGL. At this time, the chaff was still sufficiently concentrated to produce a reflectivity signature of  $\sim 22\text{ dBZ}$  within the non-uniform cloud of  $\sim -10 - +14\text{ dBZ}$  at this altitude. However, no enhanced reflectivity due to crystals from seeding was detected in the chaff gaps (Fig. 9b).

Also at this time, the chaff signature was evident between  $\beta = 10^{\circ}$  and  $25^{\circ}$ , or  $\sim 2.3$  and  $4.7\text{ km}$  AGL. The chaff had spread through a 2.4 km vertical cloud volume, and some of it had ascended  $\sim 1.0\text{ km}$  above the release level in the gravity wave updraft. Single filaments of chaff nominally settle  $\sim 0.25\text{ cm s}^{-1}$ . The earliest portions of the chaff release would account for the highest altitude chaff. With settling accounted for, the ascent distance was  $\sim 1.23\text{ km}$  during the 15 min elapsed from the beginning of the chaff releases; this equates to an updraft of  $\sim 1.4\text{ m s}^{-1}$ . Clumps of chaff fibers settle faster and account for the lower reaches of the detected chaff volume; the 2.3 km vertical spread indicates a maximum chaff fallspeed of  $\sim 2.5\text{ m s}^{-1}$ , which would simulate 2 mm densely rimed crystals or graupel. (Pruppacher and Klett 1978, p. 343).

The wave updraft made substantial liquid available to activate the glaciogenic contact nuclei. Droplet concentrations of the order of  $100\text{--}200\text{ cm}^{-3}$

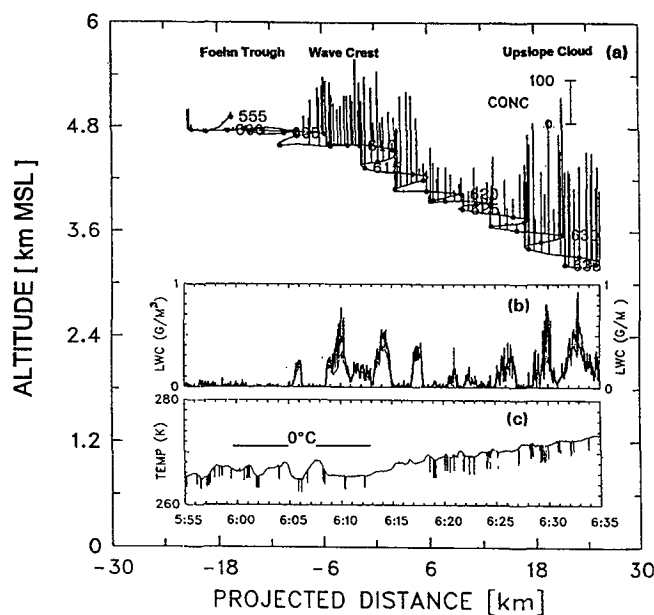


Fig. 8. Microphysical measurements from a west-to-east aircraft spiral transect and descent intersecting the foehn trough, wave crest, and an underlying upslope cloud between 0555 and 0635 UTC 6 March 1995: (a) cloud droplet concentration ( $\text{CONC}$ ,  $\text{cm}^{-3}$ ); bar scale superimposed on flight track plotted as altitude in km MSL vs. distance relative to the radar site at Cottonwood); with insets as a function of time approximately equal to the distance scale, of (b) LWC ( $\text{g m}^{-3}$ ) from a King probe (light line) and an FSSP (dark line); and (c) air temperature ( $^{\circ}\text{K}$ ; spikes are due to radio transmissions and do not indicated temperature values).

occurred with the LWCs 0.25-0.7 g m<sup>-3</sup> through the wave crest. The temperature was more consistently -8 to -9°C through the crest. Given these conditions and the well-documented placement of the seeding agent, there is no question that ice was generated by seeding in the wave cloud.

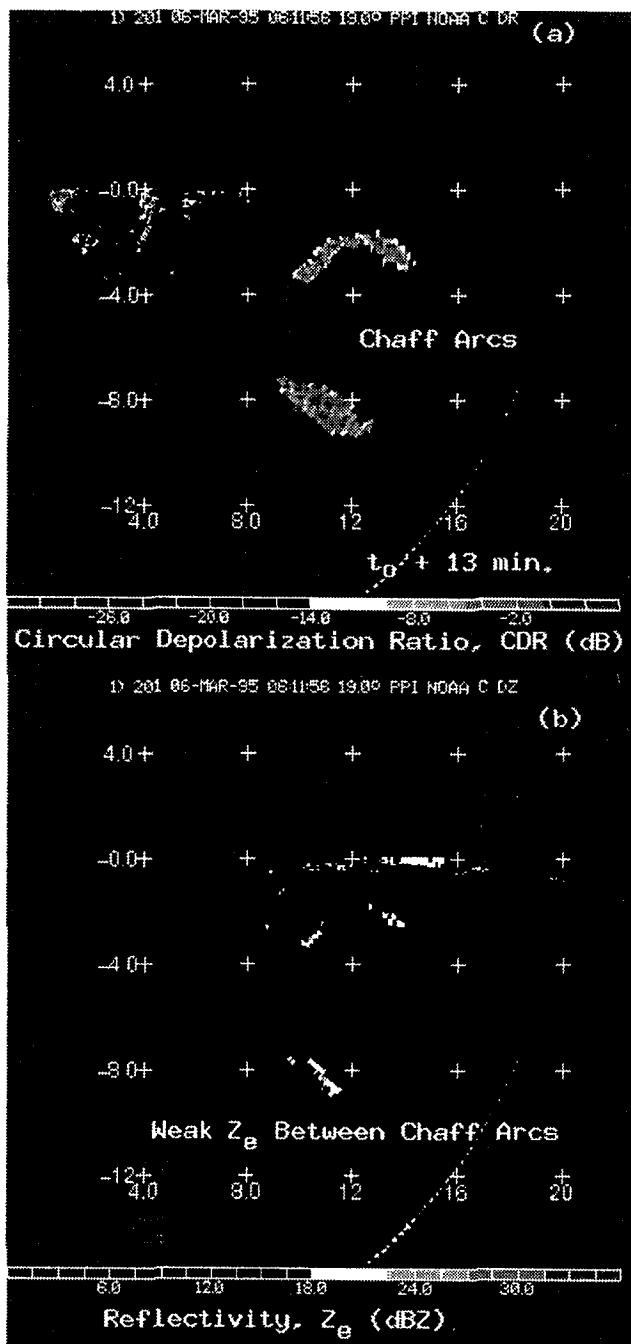


Fig. 9. Radar images for  $t_0 + 13$  min: (a) CDR (dB) of the two arcs of chaff; scale +4 – -32 dB. (b) Corresponding  $Z_e$  (dBZ) of cloud and chaff arcs. Cartesian grid is distance relative to the radar site; interval is 4 km (6 March 1995).

The first detection of what may be interpreted as a seeding signature from the resulting ice crystals on the seeded ring appeared between the chaff arcs (CDR, Fig. 10a) in the reflectivity signature in the downwind (east) gap at 062036 UTC (Fig. 10c). At  $t_0 + 22$  min, substantial time was allowed for AgI-nucleated crystals to grow to detectable sizes in concentrations above the background cloud. Indeed, the question arises, why would the ice-crystal production take so long? Contact nucleation is slow compared to other modes; it occurs continuously but gradually after release and takes on the order of 20 min to nucleate 100% of the active particles (W. Finnegan, personal communication). Also, production was likely slowed by a slow AgI nucleation rate at the -6 to -8°C temperatures, and initially by low LW contents as the seeding material (and chaff) were transported through the foehn gap before reaching the ascending condensation zone of the wave. At this detection, the circle of reflectivity in the gap between the chaff arcs was enhanced by about 10 dB over the surrounding cloud (Fig. 10c).

In subsequent scan volumes,  $Z_e$  was enhanced in both gaps between the chaff arcs (such detection depended strongly on radar elevation angle). For example, at 062810 UTC ( $t_0 + 30$  min) at altitude ~3.4 km AGL, the chaff arcs are still lucidly identified in the CDR between ~-4 and -12 dB Fig. 10b, and the enhanced  $Z_e$  in both gaps is evident in Fig. 10 d. On its downwind (east) edge, the seeding ring was merging with cloud of naturally enhanced reflectivity, but the seeding signature was also lucidly visible in the upwind chaff gap, where  $Z_e$  exceeded that of the surrounding cloud by as much as 15 dB.

Figure 11 summarizes the chaff tracking and observed radar reflectivity enhancements in the seeded ring for the entire case study. The position of the ring was established by the chaff arcs, observed as  $CDR \geq -14$  dB as they advected eastward. The highest altitude of positively identified chaff was noted to initially increase, then decrease with time, indicating passage through the wave and settling, as shown by the line with the interspersed letter C (for "chaff") in the figure.

Figure 11 also shows the vertical extent of the zone of enhanced reflectivity in the seeded ring, as a function of time (shaded area). To isolate this indicated seeding effect, the positions of the seeded arcs along the circle, in the gaps without chaff, were identified by projecting the curves of the chaff arcs through the whole seeded path, with consideration for the configuration of the initial near-circular aircraft track. The maximum reflectivity gradient across these

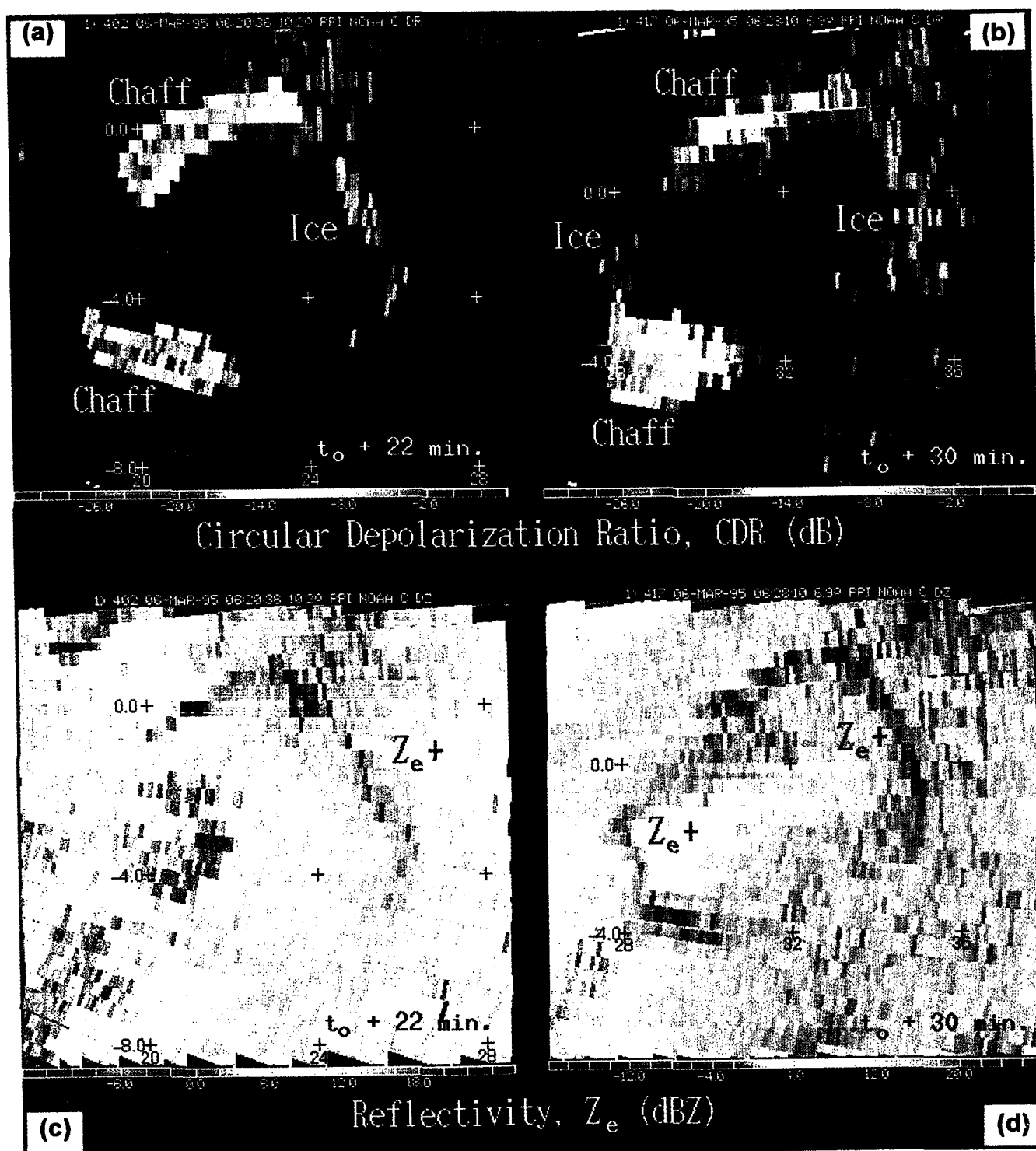


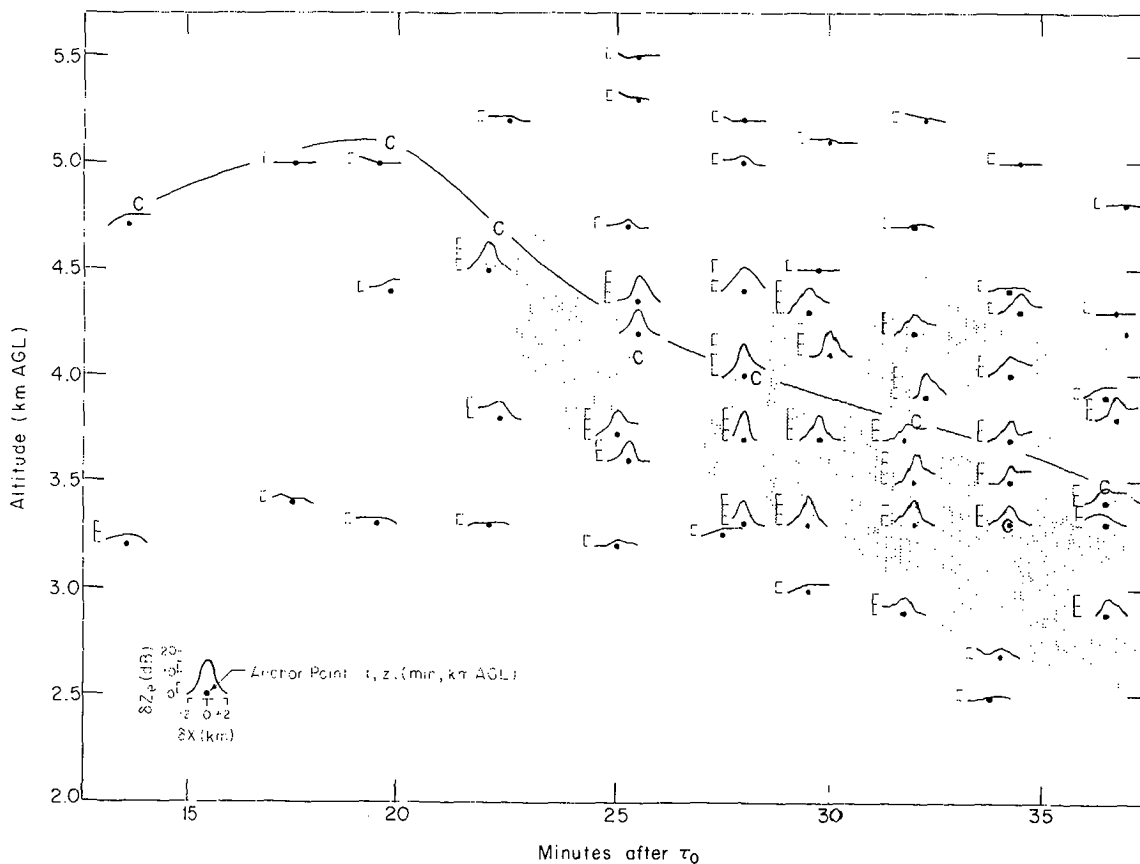
Fig. 10. (Color plate). In the top pair of radar images,  $CDR \geq -14$  dB within the scale of  $+4 \geq CDR \geq -32$  dB shows the two arcs of chaff at (a)  $t_0 + 22$  min and (b)  $t_0 + 30$  min;  $CDR \approx -27 \pm 3$  dB along the seeded circle between the chaff arcs indicates pristine, new ice crystals from seeding (noted as "ice"). The corresponding bottom pair of images (c, d) shows reflectivity within a scale of  $-20 \leq Z_e \leq +28$  dBZ and enhancements thereto (noted by " $Z_e+$ ") around the seeded circle, including the seeded path between the chaff arcs, where such enhancements also indicate increased ice crystal concentrations due to seeding. Cartesian grid with 4 km interval shows the distance relative to the radar site (6 March 1995).

north-south parts of the circle with seeding but no chaff was determined on approximately east-west line transects at positions of -2, -1, 0, +1, and +2 km from the seeded path on the circle. The minimum reflectivity along this transect was regarded as the background level, and this value, in dBZ, was subtracted from those at the other four positions which transected the seeded ring. Thus, the reflectivity difference,  $\delta Z_e$  (dB), was determined at each of five positions along each transect across the seed-only track (of course, this value was zero at the position of minimum reflectivity). The resulting individual, spatial distributions of  $\delta Z_e$  along the transects across the seeded arcs are presented as a function of time in Fig. 11, to show the enhancement of reflectivity on the seeded circle as peaks in the transects across the seeding path.

Assuming that  $\delta Z_e \geq 10$  dB occurring on the quasi-circular seed-only track—but not elsewhere in the immediate vicinity—is evidence of reflectivity enhanced by ice generated from seeding, the seeding signature first identified at  $t_0 + 22$  min as in Fig. 10c, is indicated in Fig. 11 between ~3.8 and 4.5 km AGL; this altitude range correlates well with the initial seeding altitude, allowing for the lift in the wave.

As noted earlier, the rise and subsequent descent of the top of the highest detectable chaff is indicated by the line connecting the "C's" in Fig. 11. After loft in the updraft, the top of the chaff descended faster and in time separated from the top of the  $\delta Z_e$  seeding signature, suggesting that the chaff settled somewhat faster than some of the nucleated ice crystals. This is physically probable. Nevertheless, Fig. 11 shows that the cloud volume with seeding signature deepened with time as the base of the seeding signatures descended, as expected with falling crystals. It is possible that the chaff would rime and increase its terminal velocity, but the same would happen with ice crystals, so any difference is assumed to be negligible. Thus the shaded area in Fig. 11 indicates the deepening with time of a snow plume from seeding, which was about 1.5 km deep ~35 min after the release of the AgI, when the seeding signature ( $\delta Z_e$ ) began to be obscured by background

Fig. 11. (Below) Time-altitude plot (minutes after  $t_0$ , km AGL) of radar reflectivity enhancement of the seeding ring in the gaps between the chaff arcs. Note Key and text to interpret reflectivity transects used to make this plot. Curve connected by "C's" shows highest altitude of positive chaff identification ( $CDR \geq -14$  dB). The shading identifies the envelope of time and altitude where reflectivity was enhanced on the seeded circle by ~10 dBZ or more above minimum background along the transects.



reflectivities. During this period, the seeded circle advected about 40 km to the northeast of the location where the cloud was seeded, indicating that the snow was deposited at the edge of the Mogollon rim 35-45 km east-northeast of the Cottonwood radar site.

This analysis based on  $Z_e$  is supported by some observations of an enhanced CDR that can be attributed to seeding-generated ice crystals. As noted above, Figs. 10a and b show the CDR signatures at 0620 UTC ( $t_0 + 22$  min) and 0628 UTC ( $t_0 + 30$  min), respectively. Not only the chaff was detected (as  $CDR \geq -14$  dB), but also a CDR signature of  $\sim -26 \pm 3$  dB appeared in the gaps between the chaff tags, along the seeded ring. The radar antenna elevation angles for these observations were  $10.2^\circ$  and  $6.9^\circ$ , respectively. In Fig. 10a, an enhanced CDR was evident along the seeding circle within coordinates  $X \approx 25$ -26 km,  $Y \approx 0$ -5 km; this position is in the eastward gap between chaff tags. In Fig. 10b, CDR was enhanced in both gaps between the tags, and most of the full seeding circle was evident.

A CDR signature of the order of -23 to -27 dB, at low radar elevation angles, is indicative of pristine columnar ice crystals, solid columns in particular, according to scattering calculations by Matrosov (1991). Depolarizations at such values by crystals are, fortunately, quite separable from chaff (whereas depolarization of the signal by planar crystals, for example, would be very similar to chaff at the low radar elevation angles). Although a shorter wavelength radar would afford better detectability of small ice crystals emerging from the seeding nucleation, the position and magnitude of the CDR signatures in the ring indicate that this enhanced depolarization is due to the same hydrometeors that also caused the enhanced reflectivity in the ring. There are patches of cloud with some CDR signatures from other particles, but the patterns of the signatures, filling the path along the ring of seeding, are in themselves quite convincing evidence of ice crystals from the seeding process. Since for chaff,  $CDR \geq -14$  dB and usually  $CDR \geq -5$  dB, a re-scaling of CDR in Fig. 10b to the -22 to -32 dB range eliminated the chaff signature and isolated the signatures of the ice crystal within chaff arcs as well as between the chaff arcs. The CDR values of  $\sim -28$  -  $-21$  dB in Fig. 12 within the areas of the chaff tags and between them indicate enhanced ice within the chaff tags as well as between them, as it should be since the whole ring was seeded.

After seeding and chaff release, the aircraft continued to circle and attempted to stay with the seeded plume, although a post-facto examination

indicates it gradually descended below at least the core of the plume. Ice crystal imagery from the PMS 2D-C probe on the aircraft showed columnar crystals occurring by 0625 UTC ( $t_0 + 27$  min; Fig. 13). The crystals imaged appeared to be of a transitional solid column-needle growth habit, which is in accord with the cloud temperatures of  $\sim -6^\circ\text{C}$  in the foehn trough where seeding took place, and  $\sim -8^\circ\text{C}$  through the crest of the wave where crystal growth was promoted. Prior to that, small crystals of undecipherable types were emerging. Some graupel can also be noted in Fig. 13. As noted above, the wave cloud passing through the foehn trough and into the updraft already contained ice. Polarization studies with the accompanying  $K_a$ -band radar from the storm event before and after the seeding experiment indicate that the ice passing through the trough was dominated by columnar crystals which were transformed into more spherical, less depolarizing forms, presumably by riming to graupel with liquid condensed in the wave updraft; such crystal detection and transformation is documented by Reinking et al. (1996, 1999). Thus both columnar crystals and graupel are likely responsible for much of the background reflectivity across the field of observation. However, since the conditions for formation were the same for the ice nucleated by seeding material, the background does

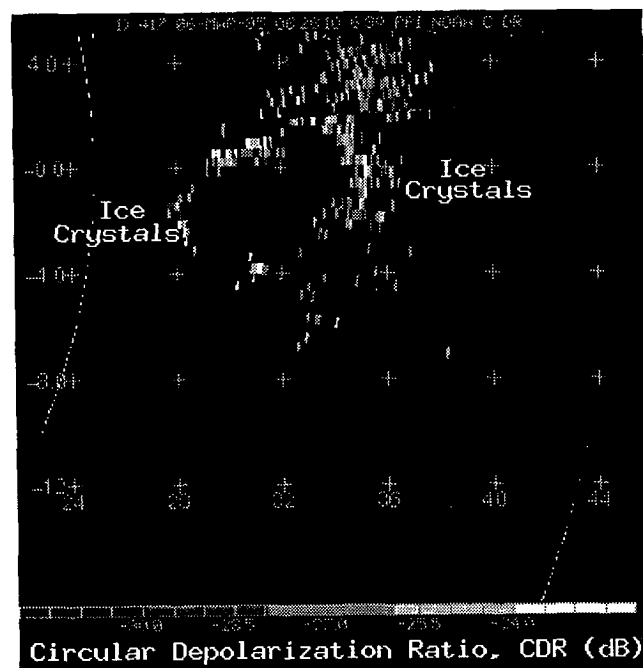


Fig. 12. Radar image of CDR (dB) re-scaled to a range of -22 to -32 dB to delete the signature of chaff and capture the signatures of pristine columnar ice crystals for  $t_0 + 30$  min, corresponding to Fig. 10b. Ice crystals around the entire seeded ring are indicated.

not preclude enhancement of ice in the form of columnar crystals and then formation of graupel by the same processes as a result of seeding, and thus appearing along the seeded ring.

A more thorough analysis of the aircraft sampling relative to the seeding event may further clarify the ice processes and seeding effects, and is the subject of a separate study. Here, the objective of demonstrating the utility of chaff tagging has been accomplished.

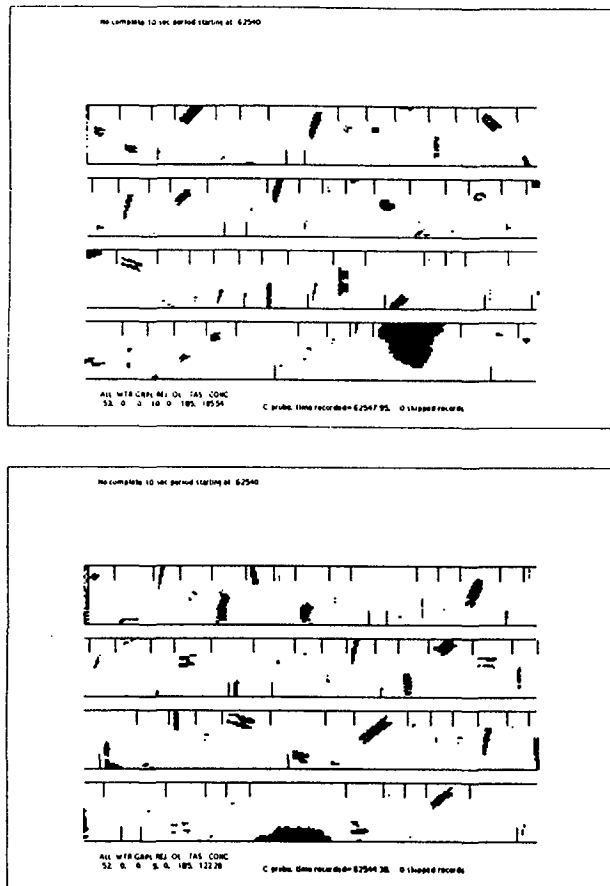


Fig. 13. PMS 2D-C images of graupel and columnar ice particles from aircraft samples in the downwind reaches of the wave cloud at 0625 UTC (sample volume width: 800  $\mu\text{m}$ ).

## 6. CONCLUSIONS

To measure transport and dispersion in cloud and simultaneously examine unambiguously the microphysical evolution in the same cloud volume, a refined approach to TRACIR has been devised. The modified approach is to tag but not fill the cloud

volume with chaff. Chaff tagging marks cloud parcels, allowing their transport and mixing to be followed while leaving the treated cloud volume between or adjacent to the tags open for radar examination of the hydrometeor evolution. Some experimental designs for chaff tagging have been outlined for stratiform/wave clouds and cumuliform clouds. The two case studies in storm-embedded wave clouds demonstrated the principles of chaff tagging.

In one, parallel lines of chaff were released to bracket a line of hygroscopic seeding in a wave cloud system confounded by underlying convective cells. The lines and their evolution were clearly tracked in the chaff CDR signatures, which could be followed for nearly 1 h. The hygroscopics increase drop concentrations and may widen the drop size distribution, so an enhanced reflectivity is likely the best radar parameter for finding a seeding signature. Such detection may be difficult even in uniform clouds, but the experiment was worth trying. The complexity of the cloud in this particular case, caused by the intrusion of some convection into the stratiform wave cloud, precluded finding good evidence of a line of enhanced reflectivity, and thus a seeding signature. This suggests that chaff tagging is likely to hold more promise for stratiform clouds than convective clouds, although certain methods of tagging in convective clouds should certainly not be ruled out without trials.

In another case, a purer gravity wave cloud was seeded with AgI from an aircraft along a circular path. The path was marked with arcs of chaff, and tracked with circular-polarization radar. After ~20 min, radar reflectivities indicated by their position to be enhanced by seeding were detected on the advecting circle in the gaps between the chaff. A seeding signature was taken as a reflectivity enhancement of at least 10 dB above the background cloud. The signatures persisted in the cloud for more than 15-25 minutes, identifying a deepening snow plume that was tracked to near the elevated ground of the downwind mountain rim. Notably, it was also possible to divide the scale of circular depolarization ratio, such that  $\text{CDR} \geq -14$  dB isolated the chaff and  $-32 \leq \text{CDR} \leq -22$  isolated the columnar ice crystals on the seeding ring that were evidently produced by the seeding and were documented with aircraft measurements. Aircraft-produced ice particles (APIPS) have not been considered, but any ice of such origin would have the same effect as ice from AgI and would not change the result of this demonstration.

Quantitatively, miniscule fractions of the storm volume and total precipitation were affected by this experiment, but a capability for producing,

observing, and tracking seeding effects in gravity wave clouds was effectively demonstrated.

More experiments of this type should be conducted. With chaff tagging, the assumption that seeding nucleants activate in natural clouds just as they do in laboratory clouds can be tested. Using stratiform clouds as natural laboratories, adjacent tagged circles could be seeded with differing nucleants and the results compared. For example, fast-acting vs. slow-acting chemical complexes of AgI could be compared. A measure of dilution is also possible in the radar signatures from chaff, so estimates of nucleation activity may also be derived. The tagging technique is equally applicable to following cloud parcels to determine their kinematic and microphysical evolution resulting from ingestion of natural or anthropogenic aerosols of any kind. Such chaff-tracking experiments on PBL venting by cumuli may become important, since pollution effects on rain and water resources are a rising international concern.

*Acknowledgments.* The field work was funded by the NOAA/Arizona Atmospheric Modification Program, NOAA Cooperative Agreement Number IGA 91-6111-189-1085. Supplemental funding was provided by the NOAA Office of Global Programs. K. Clark, along with co-author Bruce Bartram, engineered and operated the radar. Michelle Ryan and Brooke Olson processed the radar data, and Rachel Ames processed the aircraft data.

## REFERENCES

- Bruintjes, R., T. Clark, and W. Hall, 1993: Interactions between topographic airflow and cloud and precipitation development during the passage of a winter storm in Arizona. *J. Atmos. Sci.*, **51**, 48-67.
- Bruintjes, R., R.F. Reinking, B.W. Orr, B.A. Klimowski, and E.A. Betterton, 1996. Observational study of silver iodide seeding in a gravity wave cloud in Arizona. *Preprints, 13<sup>th</sup> Conf. on Planned and Inadvertent Wea. Modif.*, Atlanta, GA. Amer. Met. Soc., Boston, 1-8.
- Hobbs, P.V., J.H. Lyons, J.D. Locatelli, K.R. Biswas, L.F. Radke, R.R. Weiss, Sr., and A.L. Rangno, 1981: Radar detection of cloud seeding effects. *Science*, **213**, 1250-1252.
- Klimowski, B.A., R. Becker, E.A. Betterton, R. Bruintjes, T.L. Clark, W.D. Hall, B.W. Orr, R.A. Kropfli, P. Piironen, R.F. Reinking, D. Sundie, and T. Uttal, 1998: The 1995 Arizona Program: Toward a better understanding of winter storm precipitation development in mountainous terrain. *Bul. Amer. Met. Soc.*, **79**, 799-813.
- Martner, B.E., and R.A. Kropfli, 1989: A radar technique for observing the exchange of air between clouds and their environment. *Atmos. Environ.*, **23**, 2715-2721.
- Martner, B.E., J.D. Marwitz, and R.A. Kropfli, 1992: Radar observations of transport and diffusion in clouds and precipitation using TRACIR. *J. Atmos. Ocean. Technol.*, **9**, 226-241.
- Matrosov, S.Y., 1991: Theoretical study of radar polarization parameters obtained from cirrus clouds. *J. Atmos. Sci.*, **48**, 1062-1070.
- Matrosov, S.Y., R.F. Reinking, R.A. Kropfli, and B.W. Bartram, 1995a: Estimation of hydrometeor shapes and types with elliptical polarized radar signals. *J. Atmos. Ocean Technol.*, **13**, 85-96.
- Matrosov, S.Y., R.F. Reinking, R.A. Kropfli, and B.W. Bartram, 1995b: Identification of ice hydrometeor types from elliptical polarization radar measurements. *Preprints, 27th Conf. Radar Meteorol.*, 9-13 October 1995, Vail, CO. Amer. Meteor. Soc., Boston, pp. 539-541.
- Pruppacher, H.R. and J.D. Klett, 1978: *Microphysics of clouds and precipitation*. D. Reidel, Dordrecht, Holland. 714 pp.
- Reinking, R.F., 1995: An approach to remote sensing and numerical modeling of orographic clouds and precipitation for climatic water resources assessment. *Atmos. Res.*, **35**, 349-367.
- Reinking, R.F., and B.E. Martner, 1996: Feeder-cell ingestion of seeding aerosol from cloud base determined by tracking radar chaff. *J. Appl. Meteor.*, **35**, 1402-1415.
- Reinking, R.F., and B.E. Martner, 1999: Polarimetric short-wavelength radar technologies for assessing the evolution of clouds and precipitation following hygroscopic seeding. *Preprints, Seventh WMO Sci. Conf. On Wea. Modif.*, 17-22 February 1999, Chiang Mai, Thailand. WMP Report No. 31, WMO/TD 936. Sec. of the WMO, Geneva. I, 83-86.
- Reinking, R.F., J.B. Snider, and J. Coen, 1999: Influences of storm-embedded orographic gravity waves on cloud liquid water and precipitation. *J. Appl. Met.* (accepted).
- Stith, J., J. Scala, R. Reinking, and B. Martner, 1996: Combined use of three techniques for studying transport and dispersion in cumuli. *J. Appl. Meteor.*, **35**, 1387-1401.